# Reliability-Based Design Optimization of a Transonic Compressor

Yongsheng Lian*
Ohio Aerospace Institute
22800 Cedar Point Road, Cleveland, OH, 44142
Nam-Ho Kim†
Department of Mechanical and Aerospace Engineering
University of Florida
Gainesville, FL 32611

**A multi-objective, reliability-based design optimization technique of a compressor blade is proposed using response surface methods and genetic algorithms. The design objectives are to maximize the stage pressure ratio and to minimize the weight of the NASA rotor67 transonic blade, while satisfying both aerodynamic constraint and structural reliability constraint. Thirty two deterministic design variables are used to define the shape of the blade, while two random variables are used to characterize the uncertainties in material properties. Reliability analysis is performed using the second-order response surface and Monte Carlo simulation. The probabilistic sufficiency factor, which is superior to the probability of failure and safety factor in terms of accuracy in the regions of low probability of failure when calculated using Monte Carlo simulation, is used as an alternative measure of safety in reliability-based design optimization. Quadratic design response surfaces are utilized to filter the noise from the Monte Carlo simulation and also facilitate the multidisciplinary design optimization. The genetic algorithm is employed to find the Pareto-optimal solutions. To expedite the convergence and find a well-converged solution, we also use a local search. Numerical results show that with this proposed approach we**

*Senior Researcher, Member AIAA
†Assistant Professor, Member AIAA

**can obtain a reliable design with better aerodynamic performance and less weight.**

# I. Introduction

For decades, many researchers have used optimization techniques to improve the engine performance. Some focus on a specific discipline, others involve in multi-disciplines. For instance, Oyama et al.[1] minimized the entropy generation of the NASA rotor67 blade, Benini[2] improved the total pressure ratio and the adiabatic efficiency of the NASA rotor37 blade, Mengistu and Ghaly[3] performed multi-point design of compressor rotors to improve their aerodynamic performance, Lian and Liou[4,5] performed multidisciplinary and multi-objective optimization of the NASA rotor67 blade with a coupled genetic algorithm and response surface technique. In the aforementioned works, the design variables were assumed known deterministic parameters. For engine design, however, uncertainties and randomness exist in the material properties and design variables. To ensure robust and reliable designs, we need to account for these uncertainties or randomness in the optimization procedure.

Reliability-based design optimization (RBDO) is a technique to consider the uncertainty of input parameters in the design process. It provides not only the performance value but also the confidence range. On the other hand, RBDO involving a computationally demanding model has been limited by the relatively high number of required analyses for uncertainty propagation during the design process. In order to overcome this limitation, several alternatives with various degrees of complexity, such as moment- based methods[11,12] and Monte Carlo simulation (MCS), have been proposed. The moment based-methods are relatively efficient because they approximate the performance measure at the most probable point using linear of quadratic functions. However, the accuracy of these approximations is a concern when the performance function exhibits nonlinear behavior. Another drawback of moment-based methods is that they are not well suited for problems with many competing critical failure modes.[13] The MCS is a simple form of the basic simulation. It provides a powerful tool for evaluating the risk of complex engineering systems. It is widely used in reliability analysis because of its simplicity and robustness. Nonetheless, the MCS requires a large amount of analyses for a good estimation of the probability of failure, especially when the failure probability is small. And MCS can also produce noisy response.[13] Response surface approximation has the capability to handle these two problems. In addition, the use of response surface approach facilitates multidisciplinary optimizations, which face the challenges of computational expense and organizational complexity.

In this paper, a multi-objective RBDO of a NASA rotor67 compressor blade is proposed using response surface techniques and genetic algorithms. The objectives are to maximize

the stage pressure ratio and to minimize the blade weight while satisfying the constraints on reliability of maximum blade stress and mass flow rate. A real-coded genetic algorithm is used to facilitate the multi-objective optimization. The limits on reliability constraints are set up such that the probability of failure is less than $10^{-4}$. Thirty two deterministic design variables are used to determine the shape of the blade, while two random variables are used to characterize the uncertainties in material properties. In order to address the aerodynamic performance as well as the structural performance, a sequential analysis technique has been adopted in which structural deformation does not influence on aerodynamic performance. This assumption is valid when the structural deformation is small. The response surface is built based on the preselected design points. Their aerodynamic and structural performances are evaluated using high-fidelity tools. A computational fluid dynamics (CFD) tool is used to compute the aerodynamic force, which is then transferred from the CFD grid to the structural finite element grid. To ensure the conservation of energy between the flow and the structural systems, the thin plate interpolation is used as the interpolation technique.[7,23] A commercial finite element analysis program, ANSYS, is then used to compute the maximum von Mises stress at the top and bottom surfaces of the blade. The RBDO is performed on the response surface using the genetic algorithm and MCS.

## II. Problem Formulation

The studied rotor, NASA rotor67, is a low aspect ratio design rotor and is the first stage rotor of a two-stage fan. The rotor has a design pressure ratio of 1.63 at a mass flow rate of 33.25 kg/sec. The design rotational speed is 16,043 rpm, which yields a tip speed of 429 m/sec and an inlet tip relative Mach number of 1.38. The rotor has 22 blades and an aspect ratio of 1.56 (based on average span/root axial chord). The rotor solidity varies from 3.11 at the hub to 1.29 at the tip. The inlet and exit tip diameters are 51.4 cm and 48.5 cm, respectively, and the inlet and exit hub/tip radius ratios are 0.375 and 0.478, respectively. A fillet radius of 1.78 mm is used at the airfoil-hub juncture. The square root of the mean square of the airfoil surface finish is 0.8 $\mu$m or better, and the airfoil surface tolerance is $\pm 0.04$ mm.[10] Previously we performed deterministic design optimization based on the same configuration, which is controlled by 32 design variables. The blade geometry and the computational grid are shown in Fig. 1. We use $0.6 \times 10^6$ nodes to model per single passage.

Here we incorporate the information on uncertainty into the actual design problem. The

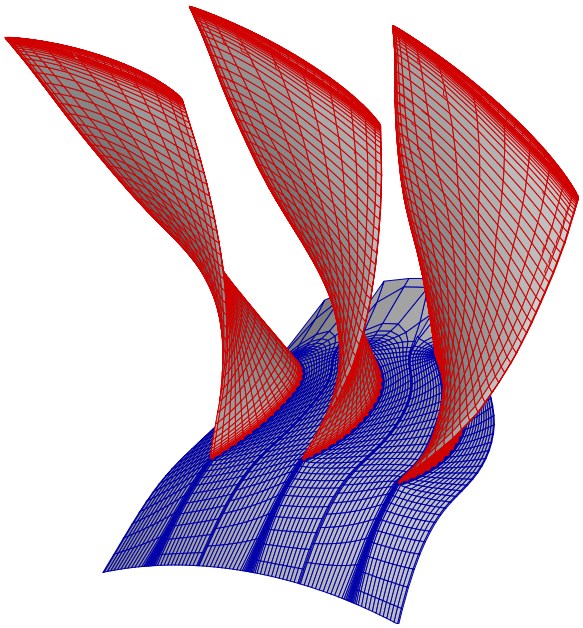

**Figure 1. Structured grid for single passage with $0.6 \times 10^6$ nodes.**

Reliability-based design optimization problem can then be defined as:

$$\text{Minimize:} \quad W \tag{1}$$

$$\text{Maximize:} \quad p_{02}/p_{01} \tag{2}$$

$$\text{Subject to:} \quad 1 - P_{sf} \leq 0 \tag{3}$$

$$|\dot{m} - \dot{m}_{\text{b}}|/\dot{m}_{\text{b}} < 0.0005 \tag{4}$$

$$\vec{d}_L \leq \vec{d} \leq \vec{d}_U \tag{5}$$

where $W$ is the blade weight; $p_{02}/p_{01}$ is the stage pressure ratio; $P_{sf}$ is the probabilistic sufficiency factor, which we will elaborate in the following section; $\dot{m}$ is the mass flow rate; $\vec{d}$ is the vector of design variables, and $\vec{d}_L$ and $\vec{d}_U$ are the lower and upper bounds of the design variables, respectively. The aerodynamic objective is to maximize the stage pressure ratio while the structural objective is to minimize the total structural weight. These two objectives are competing. This optimization problem does not have a single optimal solution, instead, it has a set of Pareto-optimal solutions, among which no solution is better than the others in terms of both objective functions. The curve formed by joining these solutions are known as Pareto-optimal front. This optimization is performed under two constraints: the aerodynamic one is to maintain a comparable mass flow rate as the baseline, the structural one is set so that the failure probability is less than a required threshold, $P_t$.

Because the blade has a very good surface finish, the impact of the randomness occurred in the design variables can be tightly controlled. Therefore, we treat all the design variables

as deterministic variables. The blade is made of Titanium (Ti-6V-4Al), whose properties are listed in Table 1. In engineering design, the probability of failure is usually based on the maximum stress failure criterion, which states that the yielding (failure) occurs when the von Mises stress exceeds the yield strength. In our test we notice that the Titanium yield limit is in the range of 786∼910 Mpa, which is much higher than the mean response of the maximum stress 4.[illegible]Mpa. There is no design violating the structural constraint if the criterion is based on the yield stress. This makes the RBDO mea[illegible]gless. For demonstration purpose, in our work we choose the endurance limit, which is the maximal stress or range of stress that can be repeated indefinitely without failure of the material. The failure criterion then states that failure occurs when the von Mises stress exceeds the endurance limit. We treat the Poisson's ratio and the endurance limit as random variables. We assume they have a normal distributions around their means. Because a normal distribution, which is valid from -$\infty$ to +$\infty$, lacks a physical interpolation, we consider the random variable as belonging to a range bounded by its mean $\pm 3\sigma$. Here $\sigma$ is the standard variation. This approach has a marginal error with a probability of 0.997 instead of 1. The distribution function of the endurance limit is plotted in Fi[illegible]. The material has a nominal density of 4510 kg/$m^3$. The Young's modulus is a random variable too, however, it does not change the value of the von Mises stress, it is therefore not factored into the reliability analysis.

**Table 1. Properties of Ti-6Al-4V, Annealed(genetic)**

| Young's Modulus [GPa] | Density [Kg/$m^3$] | Poisson's Ratio | Endurance limit [Mpa] |
|---|---|---|---|
| 116 | 4510 | 0.31∼0.37 | 529∼566 |

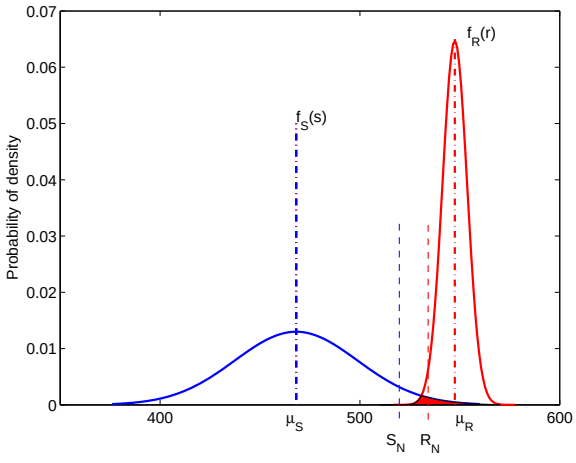


**Figure 2. Distribution functions of the von Mises stress and endurance limit.**

## III. Probabilistic sufficiency factor

In the presence of uncertainties, the maximal von Mises stress, $S$, and the endurance limit, $R$, are random variables in nature. As shown in Fig. 2 that their randomness are characterized by their means of $\mu_S$ and $\mu_R$, standard variations of $\sigma_S$ and $\sigma_R$, and their probability density functions $f_S(s)$ and $f_R(r)$. Deterministic designs require a conservative safety margin to ensure the design safety. For that purpose, a nominal safety factor defined in the following is often used

$$\text{Nominal} \quad S_F = \frac{R_N}{S_N}, \tag{6}$$

where $S_N$ and $R_N$ are the deterministic (nominal) values of the von Mises stress and endurance limit, respectively. The $S_N$ is usually below while the $R_N$ is above their respective mean value. The central safety factor, which is the ratio of the mean values of $R$ and $S$, is also commonly used in deterministic design. However, these measures may fail to provide information on design reliability. For that reason, as shown in Eq. 1, in reliability-based design, the reliability can be expressed in terms of the probability of failure

$$P(S_F \leq 1) \leq P_r, \tag{7}$$

where $S_F = R/S$ is the safety factor, $P_r$ is the required probability of failure. Fig. 3 shows the PDF of the safety factor $S_F$. The shaded area under the curve left to $s = 1$ represents the probability of failure, which has an area of $P_r$. As we will discuss momentarily, Monte Carlo simulation is often employed to evaluate the failure probability. MCS often generates noise in evaluating the failure probability due to the limit size of simulations. As we will show later that the probability of failure from MCS changes by several orders of magnitude. For some designs MCS predicts zero failure probability, which does not provide useful information in the optimization procedure. In addition, for a fixed number of simulation cycles the error associated with estimated probability of failure from the MCS increases as the probability of failure decreases. Qu and Haftka[14] compared the probability of failure, safety index, and probabilistic sufficiency factor (PSF). They found that the PSF did not suffer from accuracy problems in regions of low probability of failure when calculated using MCS and it provided a measure of safety that could be used more readily than the probability of failure or the safety index.

The concept of probabilistic sufficiency factor is introduced by Birger.[15] It is the solution to the following equation

$$P(S_F \leq P_{sf}) = P_r. \tag{8}$$

For a given problem with required probability of failure, $P_{sf} = 1$ represents that the achieved probability of failure is equal to the target one; if $P_{sf} < 1$, then the design does not meet the

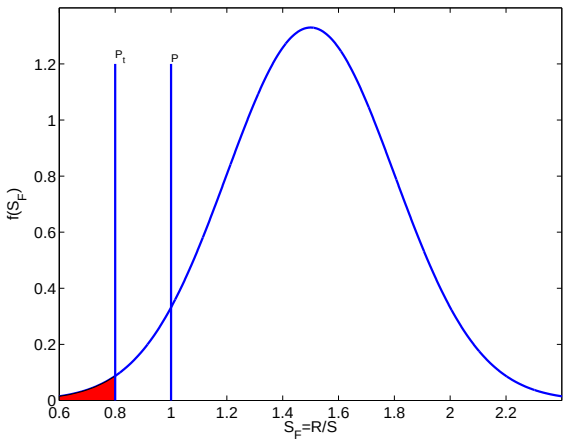


**Figure 3. Probability distribution function of the probabilistic sufficiency factor.**

safety requirement; if $P_{sf} > 1$, then the design exceeds the safety requirement. Therefore, the following two expressions are mathematically equivalent,

$$1 - P_{sf} \leq 0, \tag{9}$$

$$P(S_F \leq 1) \leq P_r. \tag{10}$$

However, Eq. 9 is advantageous in terms of accuracy.

## IV. Reliability-based optimization using response surface approximation

In reliability analysis, the first step is to decide on specific performance criterion, the random parameters, and the functional relationships among them corresponding to each performance criterion. This relationship can be written as

$$Z = g(X_1, X_2, ..., X_n), \tag{11}$$

where $Z$ represents the performance criterion, and $X_i$ is the random variable. The limit state is usually defined as $Z = 0$, which is the boundary between safe and unsafe regions in the random variable space. If the failure event is defined as $g < 0$, then the probability of failure can be calculated as

$$p_f = \int \cdots \int_{g<0} f_X(x_1, x_2, ..., x_n) dx_1 dx_2 ... dx_n, \tag{12}$$

where $x_i$ is the instantiation of $X_i$, $f_X(x_1, x_2, ..., x_n)$ is the joint probability density function (PDF) for the input random variables $X_1$,$X_2$,...,$X_n$, and the integration is performed over the failure region.

In general, the joint probability density function is practically difficult to obtain. Even if it is available, the multi- dimensional integral is difficult to evaluate. Commonly used methods are the first-order-reliability-method (FORM) and Monte Carlo simulation. Here we choose MCS because of its robustness and ease of use.

The use of approximation models is commonly practiced to reduce the computational cost. Response surface approximations are built to approximate computationally expensive problems typically using low-order polynomial. Two popular approximation methods in reliability-based design are the analysis response surface (ARS) and design response surface (DRS). The underlying distinction between the ARS and DRS is that the former is fitted to the function in terms of both deterministic variables and random variables while the latter is fitted to the function exclusively in terms of deterministic variables. In our studied problem the ARS is fitted to von Mises stress in terms of the 32 design variables and the random variable Poisson's ratio. At each design point, the probabilistic sufficiency factor is computed by the MCS based on the response surface approximation. The DRS is fitted to the probabilistic sufficiency factor in terms of the 32 design variables only. The objective functions and the structural constraint are also approximated with quadratic response surfaces. As we will see in the next that the use of response surface approximation also facilitates the multidisciplinary optimization.

## V. Monte Carlo Simulation

Estimating the probability of failure requires a multi-dimensional integral over the failure region. When the failure region is an implicit function of the performance criterion, the analytical integration would be very difficult. Moreover, the numerical integration is also impractical for high-dimensional problems. A commonly used simple method in reliability integral is the Monte Carlo simulation. MCS has evolved as a powerful tool for evaluating the reliability of complicated engineering problems. Typically, MCS consists of the following six steps:[6] (1) formulating the problem in terms of all the random variables; (2) qualifying the probabilistic characteristics of each random variable in terms of its PDF; (3) sampling the values of each random variable according to its probabilistic characteristics; (4) evaluating the problem deterministically for each set of realizations of all the random variables; (5) extracting probabilistic information from these such simulation cycles by counting the number of failed samples; (6) estimating the accuracy of the simulation.

With all the random variables assumed to be independent, MCS draws samples of the

variables according to their PDF and then feed them into the criterion model. An estimation of the probability of failure can be expressed as

$$P_f = \frac{N_f}{N}, \tag{13}$$

where $N$ is the total number of simulation cycles, i.e., solving the problem deterministically for each realization, and $N_f$ is the number simulation cycles where $g < 0$ happens. The accuracy of MCS largely depends on the number of simulation cycles. Its acceptance as an alternative reliability evaluation method mainly depends on its efficiency and accuracy. In general, this estimation accuracy depends on the true probability of failure and the number of simulation cycle. In the 95% confidence interval, the percentage error can be estimated as follows:

$$\varepsilon\% = \sqrt{\frac{(1 - p_f^T)}{N \times p_f^T}} \times 200\%, \tag{14}$$

where $p_f^T$ is the true probability of failure. In our problem we require that $p_f^T$ should be less than $10^{-4}$, with 1 million simulation cycle, the percentage error is 20%. Therefore, there is 95% probability that the probability of failure will fall into the range of $10^{-4} \pm 2 \times 10^{-5}$ with 1 million simulations.

With MCS it is straightforward to find the solution to Eq. 8. Suppose we perform $N$ analyses using the MCS around one design point, we sort the safety factor in ascending order, then the probabilistic sufficiency factor is equal to the value of the $N \times P_r$ safety factor in the sequence.

## VI. Fluid Solver and Structural Solver

A high-fidelity CFD tool, TRAF3D, is used to analyze aerodynamics of the compressor blade. TRAF3D solves the three-dimensional Reynolds-averaged Navier-Stokes equations. The space discretization uses a second-order cell-centered scheme with eigenvalue scaling to weigh the artificial dissipation terms. The system of equations is advanced in time using an explicit four- stage Runge-Kutta scheme. The two-layer eddy-viscosity model of Baldwin and Lomax is used for the turbulence closure. Details about the implementation of TRAF3D and its capability can be found in the work of Arnone et al.[8,9] and Lian and Liou.[4,5]

Following our previous work, we model the blade with quadrilateral plate element, which is a commonly used element for modeling plates, shells, and membranes. We use commercial software ANSYS to perform static structural analysis. For each element, we assume element-constant thickness and element-constant pressure. By doing this we avoid zero-thickness elements at the leading and trailing edges. The blade is structural fixed at the

hub. Therefore, the nodes at the hub are fully constrained. Each node has three translational degrees of freedom and three rotational degrees of freedom.

The multidisciplinary design optimization approach for compressor blade using high-fidelity analysis tools is presented in the work of Lian and Liou,[5] where jig-shape approach is adopted to build the compressor blade so that the structural deformation will bring the blade to its desired shape. By doing that the structural deformation on the aerodynamic performance is corrected.[20] The jig-shape approach greatly simplifies the multidisciplinary design process because now we only need to transfer the aerodynamic forces from the CFD grid to the finite element grid. The transfer of aerodynamic forces is a little bit involved because it is necessary to ensure the consistency and conservation. A thin plate interpolation method[7] is adopted for that purpose. The thin plate interpolation is derived based on the principle of virtual work it automatically guarantees the conservation of energy between the flow and the structural systems.[23] Grid sensitivity test is also performed and a grid with 2,401 elements gives a satisfactory results and is adopted. The structural system has 14,700 degrees of freedom.

## VII. RBDO Procedure

We summarize the procedure of the RBDO as follows:

- Sample design points based on both design variables and random variables with Latin hypercube sampling.
- Evaluate the design points with the high-fidelity analysis tools.
- Construct the ARS model for the maximum stress based on both the design variables and random variables.
- Perform Monte Carlo simulations based on the ARS to extract the probability sufficient factor.
- Construct the DRS models for the objective functions and constraints exclusively based on the design variables.
- Perform multi-objective optimization using a real-coded genetic algorithm.
- Improve the convergence of the Pareto-optimal front with a gradient-based method.
- Choose representative Pareto-optimal solutions to validate against the high-fidelity tools.

## VIII. Numerical Results

In the problem described in Eq. (1) there are 32 design variables and two random variables. The objective functions and the aerodynamic constraint therein are only affected by the design variables while the maximum stress is affected by the design variables and Poisson's ratio. The random variable, endurance limit, which is factored into the computation of probability sufficient factor, does not influence the maximum stress. Therefore, our sampling of design points is based on the 32 design variables and random variable Poisson's ratio. We sample 1,024 design points with the hypercube Latin sampling. These design points are evaluated using the aforementioned fluid and structure solvers. Thereafter, the ARS is built for the maximum von Mises stress based on both the design variables and the random variable. The accuracy of the response surface approximation is evaluated by statistical measures, including the adjusted coefficient of determination ($R^2_{\text{adj}}$) and the root mean square error (RMSE) predictor. The adjusted coefficient of determination is more comparable over models with different numbers of parameters by using the degrees of freedom in its computation. It measures the proportion of the variation accounted for by fitting means to each factor level. Table 2 shows the test results. The value of $R^2_{\text{adj}}$ for the maximal stress is 0.8369; the stage pressure rise has a value of $R^2_{\text{adj}}$ larger than 0.98 and a RMSE% close to zero, indicating the quadratic response surface model gives accurate representations.

Monte Carlo simulation is performed based on the built ARS. For a problem required failure probability of $1.0 \times 10^{-4}$, one million simulations are performed at each design point. After the probability of failure and probability sufficient factor are extracted, we are ready to build the DRS based on the design variables. The statistical measures are shown in Table 2. We can see that the fitting of the failure probability is poor in terms of the statistical measures. Fig. 4 shows the distribution of the failure probability, which changes several orders of magnitude over a narrow range. A quadratic response surface may not be efficient to capture the change. A high-order response surface model may be required to capture the steep variation. However, it demands more design points to fit the coefficients. In addition, we can see that more than 90% of the design has a zero failure probability. Not enough gradient information will be provided in the optimization procedure if a response surface is built based on the failure probability. If safety factor is used, we still could not avoid the large portion of flat region. On the other hand, the design response surface for the probability sufficient factor has good statistical measures. The values of $R^2_{\text{adj}}$ and %RMSE are 0.9994 and 0.002337, respectively. We plot the distribution of $P_{sf}$ in Fig. 5, which shows a smooth variation. For the studied problem with 1 million simulations and a required probability of failure less than $10^{-4}$, the error associated with the limited size of simulation is $2 \times 10^{-5}$, which is much less than that the value of 0.002637 due to the design response

surface approximation.

**Table 2. Statistical measures of the quadratic response surface approximations**

| Error Statistics | $p_{02}/p_{01}$ | $W$ | $\dot{m}$ | $S_N$ | $p_f$ | $P_{sf}$ |
|---|---|---|---|---|---|---|
| $R^2$ | 0.9949 | 0.9999 | 0.9979 | 0.9262 | 0.6638 | 0.9994 |
| $R^2_{\text{adj}}$ | 0.9888 | 0.9999 | 0.9954 | 0.8369 | 0.2572 | 0.9987 |
| RMSE | 0.564e-3 | 0.800e-5 | 0.4246e-2 | 0.1282E8 | 0.2851e-1 | 0.2637e-2 |
| %RMSE | 0.3000e-3 | 0.1175e-3 | 0.1270e-3 | 0.2761e-1 | 0.1425e3 | 0.2337e-2 |

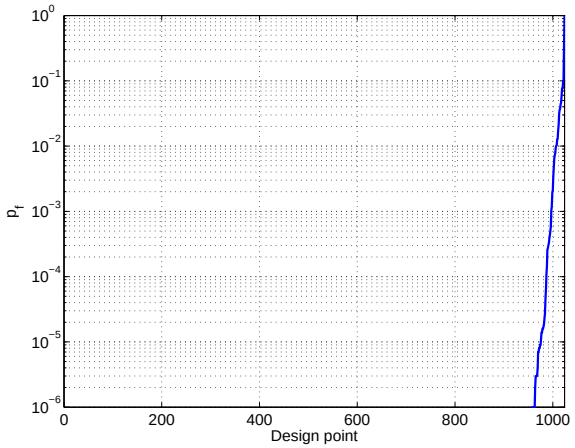


**Figure 4. Distribution of probability of failure of the 1024 design points.**

Our problem described in Eq. 1 is a multi-objective optimization problem with a set of Pareto-optimal solutions. To facilitate the optimization, we use a real-coded genetic algorithm. With the we set the population size as 320. Fig. 6 shows the solutions with different generation sizes. The convergence rate at the beginning is fast and it gradually slows down. This phenomenon is typical for genetic algorithms, which usually suffer a slow convergence rate when the optimal is approach. One remedy is to use a hybrid method. The basic idea is to switch to a gradient-based method to improve the convergence after the genetic algorithm. For that purpose we use the Design optimization tools (DOT),[24] which is software based on gradient-based methods. Fig. 6 shows that DOT does improve the convergence. Optimization is also attempted exclusively based on gradient-based methods. To do that, we transform the original problem in Eq. (1) into a single objective optimization problem by introducing weight function and DOT is employed as the optimizer. We notice that even though it obtains some solutions better that those from the hybrid method, the gradient-based method fails to identify some regions on the Pareto-optimal front. In addition, we notice that the gradient-based method is sensitive to the initial condition. The solution from

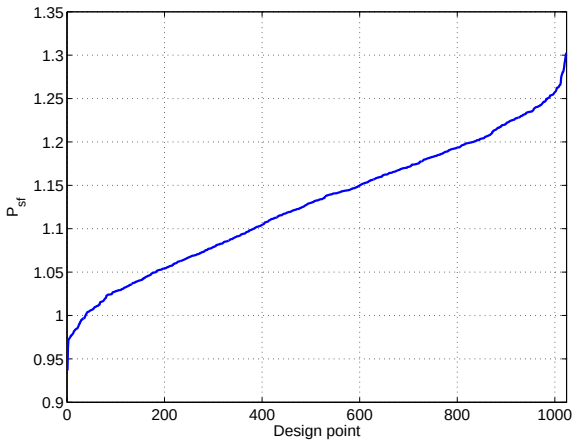


**Figure 5. Distribution of probability sufficient failure of the 1024 design points.**

genetic algorithms is also affected by the initial condition. However, the effect demolishes with the increase of generation size. We compare Pareto-optimal fronts with different initial conditions and find no evident difference at the 8000-th generation. Totally there are 693 Pareto-optimal solutions lying on the front.

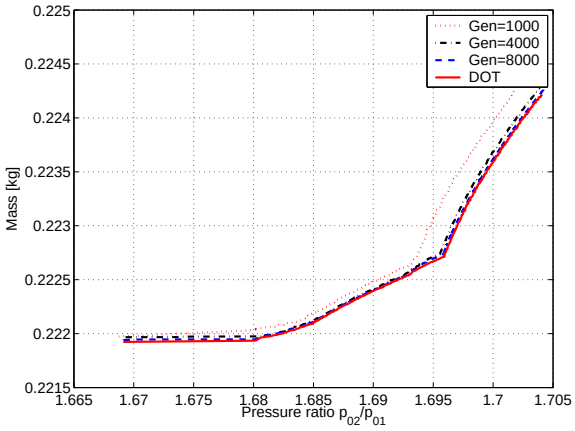


**Figure 6. Genetic algorithm convergence history and solutions from hybrid method.**

We choose 15 representative optimal design points from the Pareto-optimal front using the K-means clustering algorithm to verify against the high-fidelity analysis tools. K-means clustering is a method that chooses a set of data points from the Pareto-optimal front to accurate represent the distribution of whole date points [4,25] The distribution of the selected data points is shown in Fig. 7. We also compare the baseline with the optimal solutions. Clearly the optimization process decreases the blade weight while increasing the stage pressure ratio.

To see the impact of the accuracy of ARS, we validate the probability sufficient factor of each representative optimal design using MCS by substituting the optimal values into the

constructed ARS. This calculated PSF is compared with that predicted from optimization process. The comparison is illustrated in Fig. 8. These two set of data have a correlation coefficient of 0.9913, indicating that quadratic response surface fitting of the probability sufficient factor is an accurate approximation.

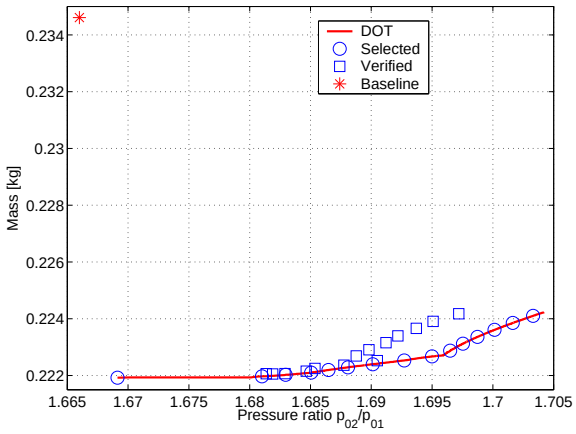


**Figure 7. Comparison of baseline with optimal solutions.**

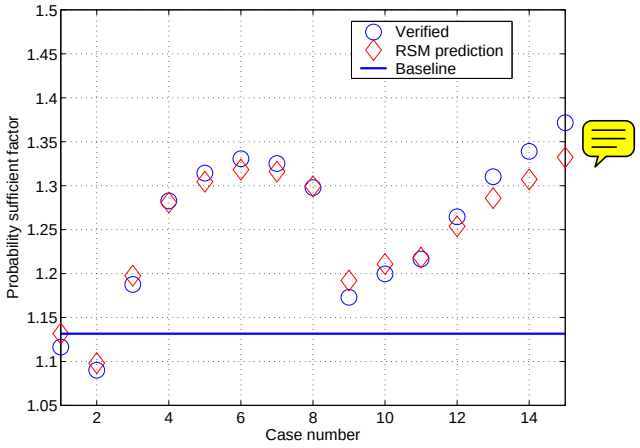


**Figure 8. Correlation of probability sufficient factor from MCS and optimization.**

## IX. Conclusions

In this paper, we demonstrated a reliability-based design optimization technique when both aerodynamic and structural performances are considered. The design uncertainty came from the material properties. Our objectives were to maximize the stage pressure ratio while minimize the blade weight. A second-order response surface model was built to make it possible to perform such a computationally intensive analysis and optimization process. A genetic algorithm was used to facilitate the multi-objective characteristics of our problem.

The reliability analysis was performed based on Monte Carlo simulation. Our numerical results showed that we could achieve a new design with lighter weight, larger pressure ratio, and reliable performance.

## X. Acknowledgements

This work is partially supported by NASA research grant NAG3-2869 under the Ultra Efficient Engine Technology Program.

## References

[1]Oyama, A., Liou, M. S., and Obayashi, S., "Transonic Axial-Flow Blade Shape Optimization Using Evolutionary Algorithm and Three-Dimensional Navier-Stokes Solver," *Journal of Propulsion and Power*, Vol. 20, 2004, pp. 612-619.

[2]Benini, E., "Three-Dimensional Multi-Objective Design Optimization of a Transonic Compressor Rotor," *Journal of Propulsion and Power*, Vol. 20, pp. 559-565, 2004.

[3]Mengistu, T., and Ghaly, W., "Single and Multipoint Shape Optimization of Gas Turbine Blade Cascades," AIAA Paper 2004-4446.

[4]Lian, Y., and Liou, M. S., "Multiobjective Optimization Using Coupled Response Surface Model and Evolutionary Algorithm," Accepted for publication at *AIAA Journal*. Also AIAA Paper 2004-4323.

[5]Lian, Y., and Liou, M. S., "Multiobjective Optimization of a Transonic Compressor Rotor using Evolutionary Algorithm," AIAA Paper 2005-1816, 2005.

[6]Haldar, A., and Mahadevan, S., *Probability, Reliability and Statistical Methods in Engineering Design*, John Wiley & Sons, Inc, New York.

[7]Duchon, J. P., "Splines Minimizing Rotation-Invariant Semi-Norms in Sobolev Spaces," *Constructive Theory of Functions of Several Variables*, Oberwolfach 1976, edited by Schempp, W. and Zeller, K., Springer-Verlag, Berlin, 1977, pp. 85-100.

[8]Arnone, A., Liou, M. S., and Povinelli, L. A., "Multigrid Calculation of Three-Dimensional Viscous Cascade Flows," NASA TM-105257, 1991.

[9]Arnone, A., "Viscous Analysis of Three-Dimensional Rotor Flow Using a Multigrid Method," *ASME Journal of Turbomachinery*, Vol. 116, 1994, pp. 435-445.

[10]Strazisar, A. J., Wood, J. R., Hathaway, M. D., and Suder, K. L., "Laser Anemometer Measurements in a Transonic Axial-Flow Fan Rotor," NASA Technical Paper 2879, 1989.

[11]Enevoldsen, I., and Sorensen, J. D., "Reliability-Based Optimization in Structural Engineering," *Structural Safety*, Vol. 15, 1994, pp. 169-196.

[12]Tu, J., Choi, K. K., and Park, Y. H., "A New Study on Reliability-based Design Optimization," *ASME Journal of Mechanical Design*, Vol. 121, No. 4, 1999, pp. 557-564.

[13]Qu. X., Haftka, R., Venkataraman, S., and Johnson, T, "Deterministic and Raliability-based Optimization of Composite Laminates for Cryonenic Enviroments," *AIAA Journal*, Vol. 41, 2003, pp. 2029-2036.

[14]Qu, X., and Haftka, R., "Reliability-based Design Optimization Using Probabilistic Factor," *Journal of Structural and Multidisciplinary Optimization*, Vol. 27, No.5, 2004, pp. 302-313.

[15]Birger, I. A., *Safety Factors and Diagnostics: Problems of Mechanics of Solid Bodies*, Leningrad, Sudostroenve (in Russian), 1970, pp. 71-82.

[16]Wu, Y. T., and Wang, W., "Efficient Probabilistic Design by Converting Reliability Constraints to Approximately Equivalent Deterministic Constraints," *Journal of Integrated Design and Process Sciences*, Vol. 2, 1998, pp. 13-21.

[17]Tu, J., Choi, K. K., and Park, Y. H., "Design Potential Method for Robust System Parameter Design," *AIAA Journal*, Vol. 39, 2000, pp. 667-677.

[18]Kim, N. H., Wang, H., and Queipo, N. V., "Efficient Shape Optimization Technique Using Stochastic Response Surfaces and Local Sensitivities," ASCE Joint Specialty Conference on Probabilistic Mechanics and Structural Reliability, July 26 - 28, 2004, Albuquerque, New Mexico.

[19]Choi, S-K, Grandhi, R, V., Canfield, R. A., and Pettit, C. L., "Polynomial Chaos Expansion with Latin Hypercube Sampling for Estimating Response Variability," *AIAA Journal*, Volume 41, No. 6, 2004, pp. 11911198.

[20]Sobieszczanski-Sobieski, J., and Haftka, R. T., "Multidisplinary Aerospace Design Optimization: Survey of Recent Development," *Structural Optimiation*, Vol. 14, 1997, pp. 1-23.

[21]Smith, M. J., Hodges, D. H., and Cesnik, C. E. S., "Evaluation of Computational Algorithms Suitable for Fluid-Structure Interactions," *Journal of Aircraft*, Vol. **37**, 2000, pp. 282-294.

[22]Brown, S. A., "Displacement Extrapolation for CFD+CSM Aeroelastic Analysis," AIAA Paper 97-1090, 1997.

[23]Liu, F., Cai, J., Zhu, Y., Tsai, H. M., and Wong, A. S. F., "Calculation of Wing Flutter by a Coupled Fluid-Structure Method," *Journal of Aircraft*, Vol. 38, 2001, pp. 334-342.

[24]DOT User's Manual, Version 4.20, Vanderplaats Research & Development, Inc., Colorado Springs, CO, 1995.

[25]Bishop, C. M., *Neural Network for Pattern Recognition*, Oxford University Press, 2003.